scientific reports

Check for updates

OPEN

Artificial embodiment displaces cortical neuromagnetic somatosensory responses

Silvia L. Isabella[1,2]✉, Marco D'Alonzo[1], Alessandro Mioli[1], Giorgio Arcara[2], Giovanni Pellegrino[3,5] & Giovanni Di Pino[1,4,5]

Integrating artificial limbs as part of one's body involves complex neuroplastic changes resulting from various sensory inputs. While somatosensory feedback is crucial, plastic processes that enable embodiment remain unknown. We investigated this using somatosensory evoked fields (SEFs) in the primary somatosensory cortex (S1) following the Rubber Hand Illusion (RHI), known to quickly induce artificial limb embodiment. During electrical stimulation of the little finger and thumb, 19 adults underwent neuromagnetic recordings before and after the RHI. We found early SEF displacement, including an illusion-brain correlation between extent of embodiment and specific changes to the first cortical response at 20 ms in Area 3b, within S1. Furthermore, we observed a posteriorly directed displacement at 35 ms towards Area 1, known to be important for visual integration during touch perception. That this second displacement was unrelated to extent of embodiment implies a functional distinction between neuroplastic changes of these components and areas. The earlier shift in Area 3b may shape extent of limb ownership, while subsequent displacement into Area 1 may relate to early visual-tactile integration that initiates embodiment. Here we provide evidence for multiple neuroplastic processes in S1—lasting beyond the illusion—supporting integration of artificial limbs like prostheses within the body representation.

Keywords Somatosensory evoked fields, Electrical stimulation, Rubber hand illusion, Magnetoencephalography, Primary somatosensory cortex, Embodiment

The sense that an artificial limb has become a part of one's body (embodiment) involves neuroplastic changes arising from multiple and sometimes conflicting sensory inputs to the brain[1,2]. However, many aspects of successfully embodying new body parts, or how this might fail remain largely unknown (as occurs in up to 44% of amputees[3], although he reasons for abandoning a prosthesis are many and varied—see[4] for a detailed discussion). Given that somatosensory feedback is crucial for embodiment[5–8], this study sought to determine the adaptive processes within somatosensory responses that accompany embodiment of an artificial limb.

Since the primary somatosensory cortex (S1) is the first cortical region reached by tactile afferent inputs, it is thought to have a central role in the acceptance of a new body part into the body schema[9–11]. Current evidence suggests that S1 is attenuated in embodiment to facilitate prioritization of visual inputs[1]. However, it remains unclear what are the *contributions* of S1 to the accommodation of an artificial limb into the body representation.

S1 is known to undergo significant neuroplasticity in response to use or environmental changes (i.e., bottom-up processes), balanced with changes in expectations (i.e., top-down processes)[12]. Neuroplastic cortical remapping following loss of function, such as losing a body part, is well-documented (e.g.[13–16]). One way to investigate this type of remapping employs peripheral electrical somatosensory stimulation, that causes a relay of activity along the somatosensory pathway towards the cortex (e.g.[17]). Signals at specific latencies are known to result from activity within different structures. The first cortical signal after peripheral stimulation of the wrist at about 20 ms (N20 or m20 of the somatosensory evoked potential or field, SEP or SEF) reflects direct and indirect effects of thalamic input to Brodmann area (BA) 3b within S1[18]. Area 3b has relatively small and well-defined receptive fields, responsible for detailed analysis of tactile stimuli, and precise localization of the stimulus on the body map. Following this, outputs from BA3b and the thalamus arrive to BA1 as early as 25 ms

[1]NeXT: Neurophsyiology and Neuro-Engineering of Human-Technology Interaction Research Unit, Universita' Campus Bio-Medico di Roma, Rome, Italy. [2]San Camillo IRCCS Research Hospital, Venice, Italy. [3]Epilepsy program, Schulich School of Medicine and Dentistry, Western University, London, ON, Canada. [4]Fondazione Policlinico Universitario Campus Bio-Medico di Roma, Rome, Italy. [5]These authors contributed equally: Giovanni Pellegrino and Giovanni Di Pino. ✉email: s.isabella@unicampus.it

(P25), in which there are larger receptive fields that integrate sensory inputs from adjacent areas of the body, for complex perceptual judgments such as object recognition[19–22]. Interestingly, it has recently been found that BA1 was more responsive to tactile stimulation when visual information was included[23]. While it is known that visual information is essential for artificial limb embodiment[24], the study by Rosenthal and colleagues points to the specific involvement of BA1 in visuo-tactile integration for successful embodiment.

The most-studied cortical responses to somatosensory stimulation occur at early (20–50 ms) and mid-latencies (50–100 ms). Although the effect of embodiment on displacements of the early-latency components has not been studied, there are interesting findings for the mid-latency component which reflect the interaction between several brain regions that convey complex stimulus information and are generally considered to represent higher cognitive processes in comparison with shorter-latency responses[25–27]. Among these mid-latency responses, an important study found evidence for neuroplastic cortical remapping following the addition of a body part: displacement of the m60 source was observed during the illusion of having a third arm[28]. However, effects of embodiment on displacements of early-latency S1 responses remain to be determined.

Early-latency cortical responses related to stimulus processing are linked to the inflow of sensory information, and they are subject to state dependant changes. For example, a displacement of the source of m20 activity as well as the source at about 50 ms (m40) (BA3b and 1, respectively) was observed following disuse by anesthesia[17]. The displacement of the m40 was similarly observed due to long term use in violin-players[29]. This use/disuse displacement in early SEF sources is a neuroplastic change that may be an important mechanism underlying changes to the body representation. These early-latency responses (20–50 ms), reflecting initial stimulus processing, have been shown to contain most of the clinically relevant cortical somatosensory response components within S1[30,31]. For example, only components within these latencies are impacted by astereognosis[32] (inability to identify objects by touch), and thus will be the focus of the current study. Displacements at the earliest latencies could point to a functional contribution of basic fundamental somatosensory processes (e.g., stimulus encoding) within S1 to successful embodiment.

To study the integration of an artificial limb within the body representation and its neural correlates, the Rubber Hand Illusion (RHI) is often employed in healthy adults and in amputees[33–35]. In this paradigm, the participant experiences an illusion of owning the fake hand (i.e. embodiment) that begins within seconds. The illusion occurs when the participant observes an artificial rubber hand stroked with a paintbrush by an experimenter, who synchronously strokes the subject's hidden real hand[36–38]. This illusion is thought to arise from the complex integration of bottom-up multisensory information and top-down expectations about sensory information[39].

The effects of the RHI on S1 and related somatosensory areas have been studied by measuring SEPs using electroencephalography (EEG), yielding mixed results. Several studies have found that the RHI enhanced a long-latency component at 140 ms[40,41] (N140), likely originating in the secondary somatosensory cortex[42]. One study demonstrated that the RHI reduced a mid-latency component around 50 ms[11] (P45). Lastly, only one study demonstrated effects within the early-latency components: the RHI reduced activity within the 20–25 ms time window[43] (N20-P25 component, occurring in BA3b and BA1, respectively). Although this study demonstrates a relationship between the RHI and the earliest SEPs, it remains unknown whether this attenuation of activity is accompanied by any adaptive processes to accommodate the artificial limb.

Early SEPs or SEFs provide accurate information on the location of sensory stimuli on the body, and a relative shift in SEF source location could be an adaptive process enabling successful embodiment. That is, a change in SEF source location following the RHI could underlie changes to the body schema, as might occur after loss or gain of a body part. Furthermore, it is known that this illusion relies upon top-down processes to prioritize visual somatosensory information[24]. Therefore, the question driving the current study is whether there is a relationship between embodiment and effects on somatosensory representation areas within S1. We expect to observe stronger changes in BA1, occuring *after* the earliest components at 20 ms within BA3b, thus representing embodiment effects at the onset of integrative processes within sensory cortices, that coordinate a reduction in representation of neighbouring body parts.

Most previous studies investigating neuroplasticity associated with the embodiment of an artificial limb have relied upon EEG that has insufficient spatial resolution to observe shifts in SEP sources, or functional magnetic resonance imaging (fMRI) that has insufficient temporal resolution. Thus, the current study was conducted using magnetoencephalography (MEG), having millisecond-temporal and millimetre-spatial resolution[44,45] to determine the relationship between the RHI and early-latency SEF source locations and magnitudes within S1. Similar to previous studies measuring neuroplastic shifts in S1 (e.g. [17,29]), subjects underwent neuromagnetic recordings during electrical stimulation of the little finger and thumb immediately before and after the RHI, to quantify relative changes to the main early SEF components and sources due to artificial limb embodiment. The extent of embodiment was measured using validated questionnaires[38], and correlated with neuromagnetic findings.

Materials and methods

Participants

Nineteen healthy adults participated in this experiment. All volunteers signed a written informed consent before their participation in this study. The study was approved by the local Ethics Committees (Province of Venice and Campus Bio-Medico University of Rome) and the protocols are in accordance with the latest Declaration of Helsinki (2013)[46].

Experimental procedure

The experimental procedure lasted about 30-min, and was performed as follows. All subjects completed the Edinburgh Handedness Inventory[47] to assess their hand dominance. Subjects sat upright in a comfortable armchair inside a magnetically shielded room with their eyes closed. For SEF assessments, ring electrodes were placed on the little finger and thumb (Little and Thumb, respectively) of the left hand for each subject and session during neuromagnetic recording. Using a high voltage stimulator (DS7A, Digitimer Ltd., UK), 400 stimulus repetitions (200 per finger) were delivered with the following parameters: square pulse duration 0.2 ms, interstimulus interval ranging from 250 to 270 ms and amplitude 3-times the sensory threshold. Stimulation to the little finger and thumb was randomly interleaved, with the stimulator housed outside of the magnetically shielded room.

This was conducted before (Pre) and immediately after (Post) a five-minute synchronous RHI procedure (Fig. 1A). For the RHI, subjects were instructed to place their left hand on a wooden platform, with the upper arm and shoulder covered by a towel. While the left hand was occluded from view by a vertical panel, a lifelike rubber hand was positioned next to the panel in a visible position, at a distance of 15 cm from the subject's left hand. Both the real (left) and rubber hands were fitted with nitrile examination gloves (Fig. 1B), to make the hands look similar. The experimenter instructed the participants to fixate on the artificial hand for the entire duration of the RHI procedure. During the 5-min procedure, the experimenter stroked the participant's left and the rubber hand with two identical paintbrushes at a pace of approximately 1 Hz. Importantly, just as the somatosensory stimulation, the RHI was performed within the magnetically shielded room, without removing the subject from the MEG. This was to ensure the comparability of pre- and post-RHI measurements.

Behavioural measures

To quantify the extent of self-attribution to the rubber hand, participants were provided with a nine-item questionnaire[38] (Supplementary Material) with which participants were asked to rate the extent to which the nine items did or did not apply, using a 7-point scale. For this scale, -3 meant "absolutely certain that it did not apply," 0 meant "uncertain whether it applied or not," and + 3 meant "absolutely certain that it applied." In order to control for participant suggestibility, three items in the questionnaire measure the illusion, whereas the other six items served as control for compliance, suggestibility, and "placebo effect". From this, the RHI-index is calculated as the difference between the mean score of the illusion items compared with the mean score of the control items[48,49], and serves as a quantification of the extent of embodiment experienced for each subject and condition.

A.

B.

Fig. 1. Experimental procedure and Setup. (**A**) Diagram of experimental procedure. Neuromagnetic evoked activity of thumb and little fingers electrical stimulation was collected before (Pre) and after (Post) the administration of synchronous RHI that lasted 5 min. The extent of embodiment was quantified through the RHI-index calculated from the answers to a questionnaire administered immediately following the procedure. (**B**) Rubber hand illusion setup, occurring between Pre and Post SEF procedures.

Magnetic resonance imaging

In order to localize MEG activity to each individual's anatomy, T1-weighted structural MR images were collected for each subject using a 3 T Ingenia CX Philips scanner (Philips Medical Systems, Best, The Netherlands).

Magnetoencephalographic recordings

Neuromagnetic activity was recorded using a whole-head 275-Channel CTF MEG system (VSM MedTech Systems Inc., Coquitlam, BC, Canada) in a magnetically shielded room. Data were collected at a rate of 1200 samples/s. Small coils placed at fiducial locations (nasion and preauricular points) were used with continuous head localization to monitor head position during recording. Head shapes and fiducial locations were digitized using a 3D Fastrack Digitizer (Polhemus, Colchester, Vermont, USA), which was used to co-register source images to the subject's MRI using the Brainstorm Matlab toolbox[50].

Magnetoencephalographic preprocessing and source analysis

Continuously recorded MEG data were segmented into 200 epochs of 1500 ms duration (500 ms pre-stimulus baseline), each for Little and Thumb, and for each session (Pre and Post). Epochs in which the peak-to-peak amplitude across MEG channels exceeded 3 pT during the time points of interest (− 50 to 240 ms) were automatically labeled and rejected following visual inspection, resulting in a mean of 170 epochs (SD = 27.7) for each finger and session included for analysis. Due to excessive noise for one subject, data from 120 channels were excluded, and analysis was performed on the remaining 153 channels for that subject.

Data were highpass filtered off-line at 0.01 Hz, with a band-stop filter (50, 100, 150 Hz) to remove power line noise. A non-phase shifting (bi-directional) 4th order Butterworth filter was used. Mean head position was calculated offline, and a multi-sphere head model[51] was used, implemented in the BrainWave Matlab toolbox[52]. In order to measure any differences in source location of SEFs, an event-related beamformer[53,54] with 2 mm spatial resolution was used to generate source activity images on a 3D grid (591,872 voxels, or $24 \times 18 \times 16$ cm) for averaged brain responses, also using BrainWave. This is a spatial filtering method that computes volumetric images of instantaneous source power corresponding to selected time points in the average (evoked) brain responses.

Data from Pre and Post sessions were combined for each finger to compute the data covariance used in estimating the beamformer spatial filter weights from the single trial data. In order to exclude effects from the stimulus artifact, the covariance window used was 10–240 ms from stimulus onset[54]. Pseudo-z statistical beamformer images were created every 1 ms over the period between 15 and 50 ms following the stimulus. Individual global maxima within the beamformer image across space and time were determined within this time window, and source direction was aligned across subjects, in native source space. Specifically we sought to identify canonical SEF responses at 20, 27, 35, and 45 ms within S1[55–57]. Given that, for example the m20 component may occur at slightly different latencies and source coordinates between subjects, a *component* is the label given to the peaks of activation across conditions for a between-subject average source and latency (e.g., *the m20 component*). For group averaging, spatial normalization was based on the MNI (T1) template brain, and subsequent scaling to Talairach coordinates were carried out using SPM12 (Wellcome Centre for Human Neuroimaging, London, United Kingdom). MNI coordinates of group-averaged source locations were plotted onto the ICBM152 template brain using Brainstorm.

Statistical analysis

For all acquired MEG and behavioural data, normality was tested using the Shapiro–Wilk test. If the data were not normally distributed, non-parametric statistical tests were used.

In order to confirm the induction of the illusion, we calculated the RHI-index as the difference between the mean scores of the illusion items and the mean scores of the control items. This index was used as the illusion outcome for the RHI condition.

To verify that the results of the RHI questionnaire was not due to participant suggestibility, the mean score of the three items employed to measure the illusion was compared with the mean score of the six items that served to control for compliance, suggestibility, and placebo effect using a paired Wilcoxon Signed Rank test.

For each subject and session, source locations at different latencies of Little and Thumb were used to calculate their Euclidian distance in native space.

In order to determine the within-subject effects of RHI on the Euclidian distance between SEF source locations we conducted a 2-way repeated measures ANOVA with two factors (session (2 levels: Pre vs Post) and component (3 levels: m20, m35, m45)). For each component, planned Pre vs Post comparisons were conducted using paired t-tests comparing values.

The source activity for each component evoked by the electrical stimulation was quantified. Since SEF peak magnitude values were not normally distributed, they were normalized using a cube-root transformation. In order to determine the within-subject effect of RHI on the SEF magnitude we ran a 3-way repeated measures ANOVA with three factors [session (2 levels: Pre vs Post), finger (2 levels: Little vs Thumb) and components (3 levels: m20, m35, m45)). For each component, planned Pre vs Post comparisons were conducted using paired t-tests comparing values.

In order to determine the presence of a relationship between embodiment measures and changes (Post- Pre) to evoked neuromagnetic activity, we conducted between-subject correlations: for each component (m20, m27, m35, m45) we correlated the change in Euclidian distance and the magnitude with RHI-index values using Spearman's rank correlation. Although we did not hypothesize any specific relational differences between fingers, and therefore averaged magnitudes for Little and Thumb, post-hoc comparisons considered them separately. All statistical tests were conducted and plots were prepared using R Statistical Software[58]. Corrections for multiple post-hoc comparisons were performed using Holm-adjusted values.

Results

All 19 subjects complied with task instructions and completed the experiment. One subject (male) was excluded from analyses due to abnormalities discovered in the structural MR image. Data from the remaining 18 (13 females, range 22–56 years) subjects were analyzed.

Rubber hand illusion index

For the RHI (conducted between Pre and Post SEF procedures), mean RHI-index values were 4.19 ± 0.38 (Fig. 2), which are comparable to values obtained in previous studies (e.g.[59]), confirming induction of the illusion (positive RHI-index values) for 17 out of 18 participants. The mean value of the illusion items was significantly higher (2.4 ± 0.15) than the mean value of the control items (− 1.75 ± 0.31; $p < 0.001$; Fig. 2). Thus, the occurrence of the RHI cannot be attributed to the suggestibility of the participants.

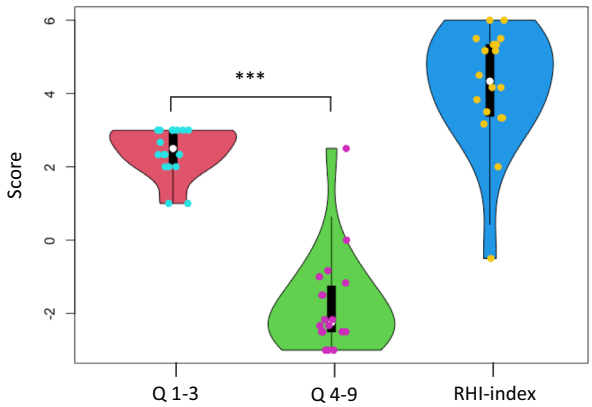

Fig. 2. Mean values obtained for the RHI questionnaire. Questions 1–3 were the illusion-related questions, while questions 4–9 were the control questions. The significant difference between these sets of questions (*** = $p < 0.001$) demonstrate that the illusion was not merely due to participant suggestibility. The RHI-index quantifies the extent of the illusion, and values are comparable with those obtained in previous studies.

Finger	Condition	Component	Latency (ms)	MNI coordinate		
				X	y	z
Little	Pre	m20	23	46	− 21	66
	Post	m20	23	47	− 18	66
Thumb	Pre	m20	23	50	− 25	62
	Post	m20	24	52	− 30	60
Little	Pre	m27	30	–	–	–
	Post	m27	30	–	–	–
Thumb	Pre	m27	28	40	− 12	72
	Post	m27	28	40	− 13	68
Little	Pre	m35	34	50	− 22	62
	Post	m35	34	50	− 22	62
Thumb	Pre	m35	35	58	− 20	58
	Post	m35	34	58	− 22	56
Little	Pre	m45	44	54	− 24	60
	Post	m45	44	54	− 22	56
Thumb	Pre	m45	44	54	− 24	60
	Post	m45	43	58	− 24	54

Table 1. Mean somatosensory-evoked response component latencies and MNI coordinates for each finger and condition, where positive x-values denote right laterality, positive y-values denote anteriority, and positive z-values denote superiority. Analyses were conducted in native space. Note that a discrete source for the m27 component for Little stimulation could not be identified.

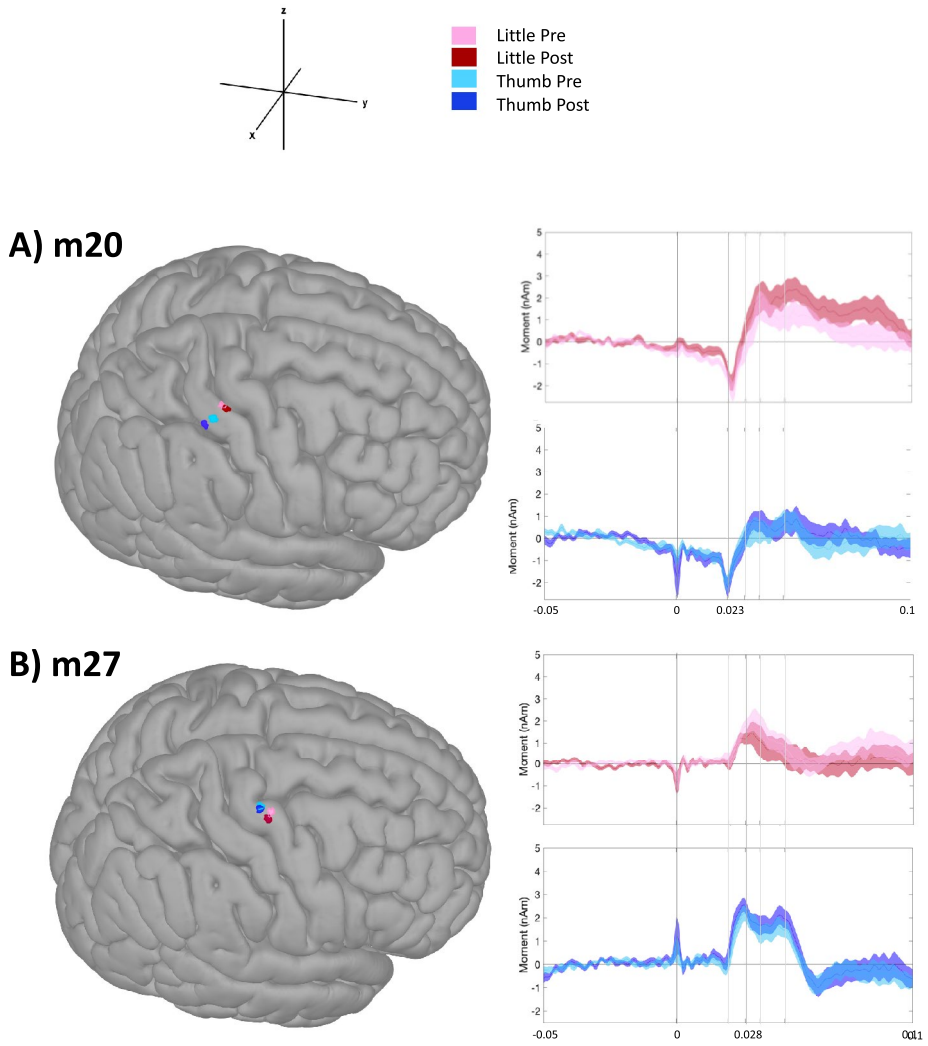

Fig. 3. Mean SEF source location, plotted onto a template brain (left) and waveforms (right) for each finger, condition, and component. MNI coordinates are summarized in Table 1, and analyses are summarized in Table 2. (**A**) SEF location (left) and activity (right) for the m20 component, with mean peak latency of 23 ms, localized to Brodmann Area 3. (**B**) SEF location (left) and activity (right) for the m27 component, with mean peak latency of 28 ms, localized to Brodmann Area 6. Little sources were estimated and plotted for visualization purposes only, and not analyzed. (**C**) SEF location (left) and activity (right) for the m35 component, with mean peak latency of 34 ms, localized to Brodmann Areas 3 and 1. (**D**) SEF location (left) and activity (right) for the m45 component, with mean peak latency of 44 ms, localized to Brodmann Area 1.

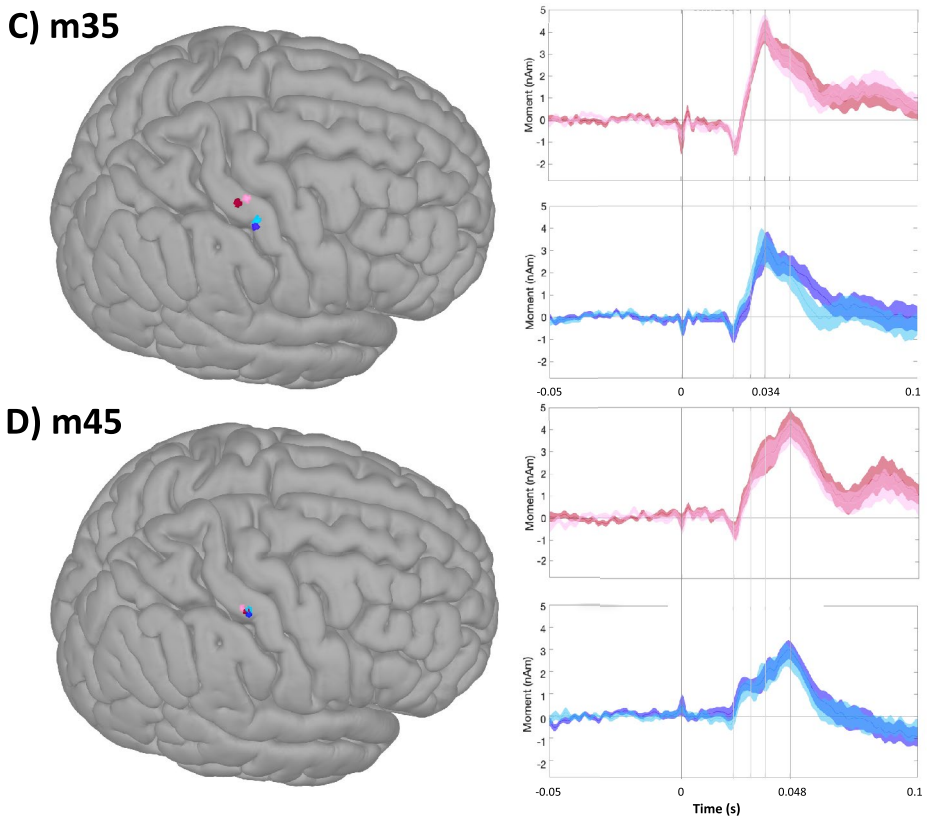

Fig. 3. (continued)

Somatosensory evoked fields: within subject comparisons

Source-level analysis revealed peak averaged activity identified at 23 ms (m20), 28 ms (m27—Thumb only), 34 ms (m35) and 44 ms (m45), the locations and latencies of which are summarized in Table 1 and displayed in Figs. 3 and 4. Although the beamformer provided a clearly identifiable source of the m27 for Thumb (Pre and Post), there was no discrete m27 source for Little (Pre or Post) and therefore was not analyzed any further. This is likely due to the proximity of the m27 for Little to its m35 source (i.e., compare Fig. 3B, C). For Little and Thumb, the m20 shifts were observed to be in opposite, anterior–posterior directions, whereas the m35 shifts were observed to mainly be in a similar, posterior direction (Fig. 4).

The analysis of the within-subject impact of RHI on SEF source Euclidian distances was performed for all subjects that experienced the illusion. This analysis revealed the presence of significant main effects of session (Pre, Post: $F(1,16) = 6.01$, $p = 0.026$, $\eta_p^2 = 0.26$) and component (m20, m35, m45: $F(1,16) = 5.416$, $p = 0.009$, $\eta_p^2 = 0.24$), with no interactions ($p = 0.52$) (Table 2, Fig. 5). Planned comparisons revealed a trend towards an increase in Little-Thumb Euclidian distance for the m20 component ($p = 0.15$), reaching statistical significance for m35 ($p = 0.017$), but not for m45 ($p = 0.35$). Next, the repeated measures ANOVA conducted on peak magnitudes across components did not reveal a statistically significant main Pre-Post effect ($F(1,16) = 0.062$, $p = 0.81$).

Somatosensory evoked fields—rubber hand illusion-index: between subject correlations

In order to investigate between-subject relationships between the parameters chosen to quantify changes in S1 activity and the extent of embodiment achieved through the rubber hand illusion procedure, RHI-index was correlated with: (i) the change in Euclidian distance (with positive values indicating a greater distance after the RHI), and (ii) the average change in source magnitude (with negative values indicating greater reduction in signal strength after the RHI) for each component. For the m20, the Pre-Post change in Euclidian distance and magnitude correlated with the RHI-index (Euclidian distance: Spearman's rho = 0.49—moderate correlation, $p = 0.02$; peak magnitude: Spearman's rho = – 0.42—moderate correlation, $p = 0.04$; Fig. 6 and Table 3). No other planned correlations were significant. Post-hoc analyses revealed that the relationship between the RHI and the m20 magnitude was mainly driven by a reduction in activity for the Little finger (Spearman's rho = – 0.61—moderate correlation, $p = 0.008$, $< p_{Holm}$ of 0.01), and not for the Thumb (Spearman's rho = -0.01—no correlation, $p = 0.97$). Given this finding, a similar post-hoc analysis for individual finger m35 magnitude revealed a relationship between the RHI and a decrease in m35 Thumb magnitude (Spearman's rho = -0.61—moderate correlation, $p = 0.007$, $< p_{Holm}$ of 0.008) was found, but not for Little (Spearman's rho = 0.28, $p = 0.26$).

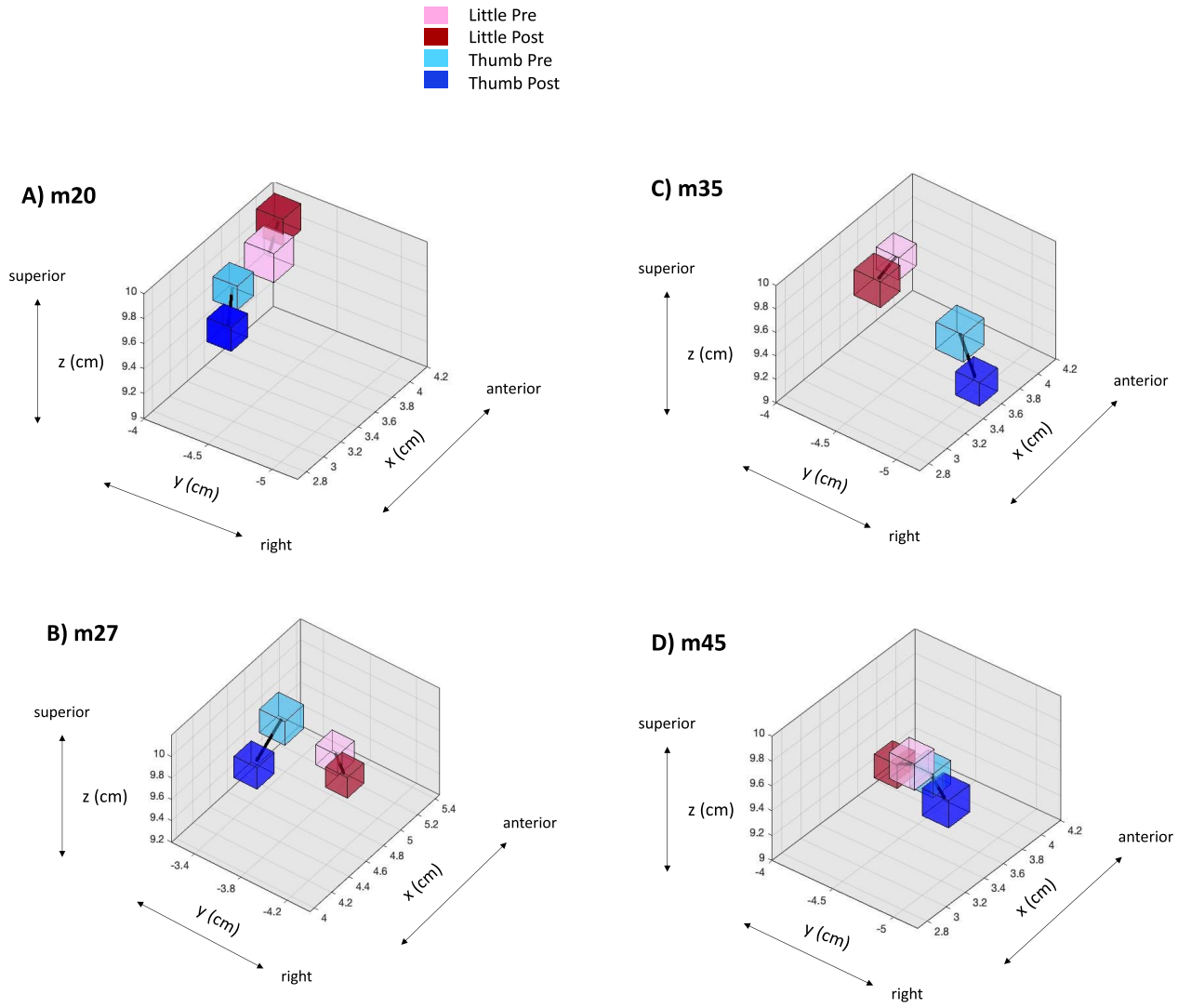

Fig. 4. Mean SEF source location, plotted in native space for each finger, condition, and component. Shape volume corresponds to the standard error across subjects. (**A**) SEF location for the m20 component, (**B**) m27 component, (**C**) m35 component and (**D**) m45 component. Note the change of axis values for (**B**) only, in the motor cortex.

	Euclidian distance (cm)	
Latency	Pre (SD)	Post (SD)
m20	1.61 (0.55)	1.84 (0.86)
m27	–	–
m35	1.27 (0.53)	1.66 (0.55)
m45	1.12 (0.54)	1.19 (0.73)

Table 2. Mean Euclidian distances between Little and Thumb SEF neuromagnetic sources, for each component for all subjects that experienced the RHI illusion (positive RHI-index). Note that m27 was excluded from statistical analyses, as described in the text.

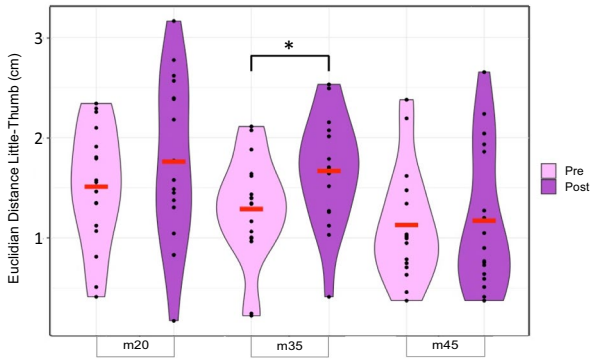

Fig. 5. Mean Euclidian distances between Little and Thumb SEF neuromagnetic sources, for each component, with Pre on the left and Post on the right. Individual values (black) and group mean (red) are plotted. Analysis of variance revealed a main effect of session (Pre vs Post: $p = 0.019$) and component (m20, m35, m45: $p = 0.026$). Planned comparisons revealed a significant increase in Euclidian distance for the m35 component ($p = 0.017$).

Discussion

Most research to date on S1 activity during the RHI points to a reduction of SEPs, thought to reflect a prioritization of visual over somatosensory information. The current study investigated the early neuroplastic processes underlying how new body parts are accommodated by the sensory cortex. We observed a change in Euclidian distance between Little and Thumb sources across BA3b and BA1, with a statistically significant within-subject displacement occurring for the m35 component. These results support our hypothesis for a neuroplastic shift at latencies beyond the m20, reflecting integration processes, especially visuo-tactile integration known to be important for the RHI and occurring in BA1[23,24]. Furthermore, different neuroplastic shifts predicted the extent of rubber hand embodiment: between-subject MEG-illusion correlations of moderate strength were observed between the RHI-index (quantifying the extent of the illusion) and the m20 component within BA3b across two parameters: (i) an increase in Euclidian distance, and (ii) the reduction in the magnitude of Little activity. An additional correlation was found between the RHI-index and the magnitude of Thumb activity for the m35 component. These differences across Brodmann areas, latencies, and fingers reveal a highly complex relationship between S1 and embodiment.

The rubber hand illusion causes a shift in somatosensory evoked field source for early components

The effect of the RHI on source localization of early SEF components was of critical interest in the current study. The timing and locations of each SEF component are consistent with previous literature[17,60], including from invasive human recordings[61]. That Thumb sources are represented relatively more posteriorly in the postcentral sulcus than Little is likely due to more distal positioning of the stimulating ring along the Thumb (on the middle phalanx, as opposed to the proximal phalanx for Little), as it has been shown that distal phalanxes are more posteriorly represented than proximal phalanxes[62]. The Euclidian distances between Little and Thumb sources (averaged across subjects) ranged between 1.19 and 1.84 cm (Table 3), consistent with previous studies[17,61,63–65].

We expected a change in Euclidian distance for the m35 component but not for the m20 component. This is because we were anticipating neuroplastic changes at the level of sensory integration that would furthermore correlate with the extent of embodiment. Although we expected this distinction between m20 and m35 components, it is very intriguing that the illusion measure correlated between-subjects only to the m20 displacement, and not the m35 displacement. It is notable that the magnitude of within-subject m20 displacement was nearly as large as the displacement for m35 (0.28 vs. 0.36 cm, respectively), but with higher variance (mean SE 0.22 vs. 0.16 cm, respectively). Thus, this variance that prevented within-subject statistical significance, that also *caused* the between-subject correlation, was related to differences in the extent of embodiment. This is an important consideration for future studies such as those using RHI that have high inter-individual differences.

Furthermore, the current results likely arise from a functional dissociation between the m20 and m35 components. That is, the SEF source displacement was larger (and more consistent) for the m35 than for the m20, but was not the displacement that correlated with the extent of embodiment. This additionally means that the stronger SEF source displacement for the m35 must have a different function from the relatively weaker SEF source displacement for the m20. As far as we are aware, these results provide the first evidence for multiple functional roles for SEF source displacements within S1.

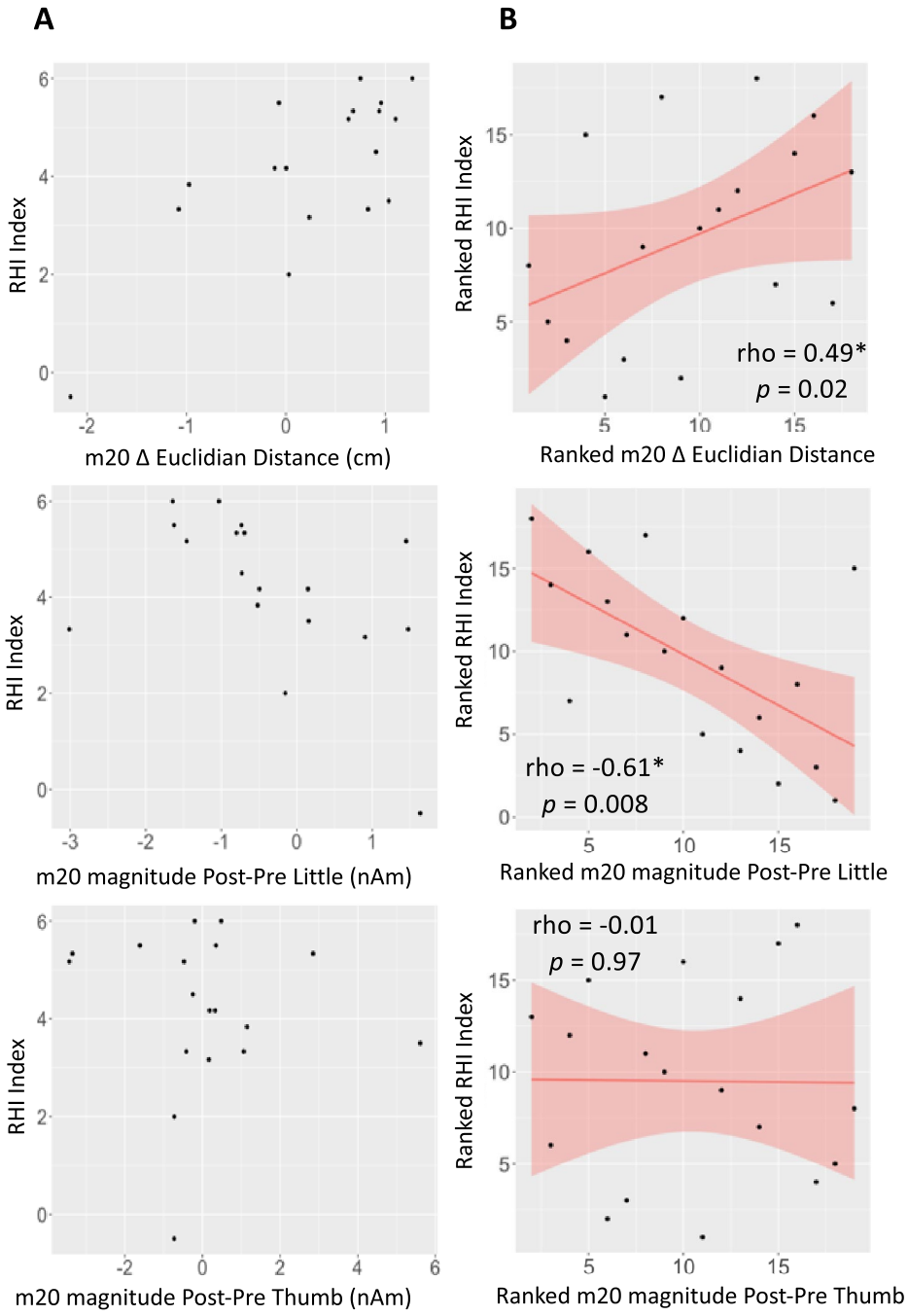

Fig. 6. Comparisons between RHI-index and (**A**) m20 original values, (**B**) m20 ranked values, (**C**) m35 original values, and (**D**) m35 ranked values. Neurophysiological measures are presented as follows: (**Top**) Change in Euclidian Distance, Post–Pre; (**Middle**) magnitude for Little, Post—Pre; (**Bottom**) magnitude for Thumb, Post – Pre. Since the data are not normally distributed, the statistical tests were conducted using ranked data (**B** and **D**). Significant correlations were found between ranked RHI Index and ranked changes in m20 Euclidian distance (**B-Top**, Spearman's rho = 0.49–moderate correlation, $p = 0.02$), m20 Little magnitude (**B-Middle**, Spearman's rho = − 0.61—moderate correlation, $p = 0.008$), and m35 Thumb magnitude (**D-Bottom**, Spearman's rho = -0.62–moderate correlation, $p = 0.007$), where positive values denote *increases* after RHI. Significant correlations are marked with an asterisk.

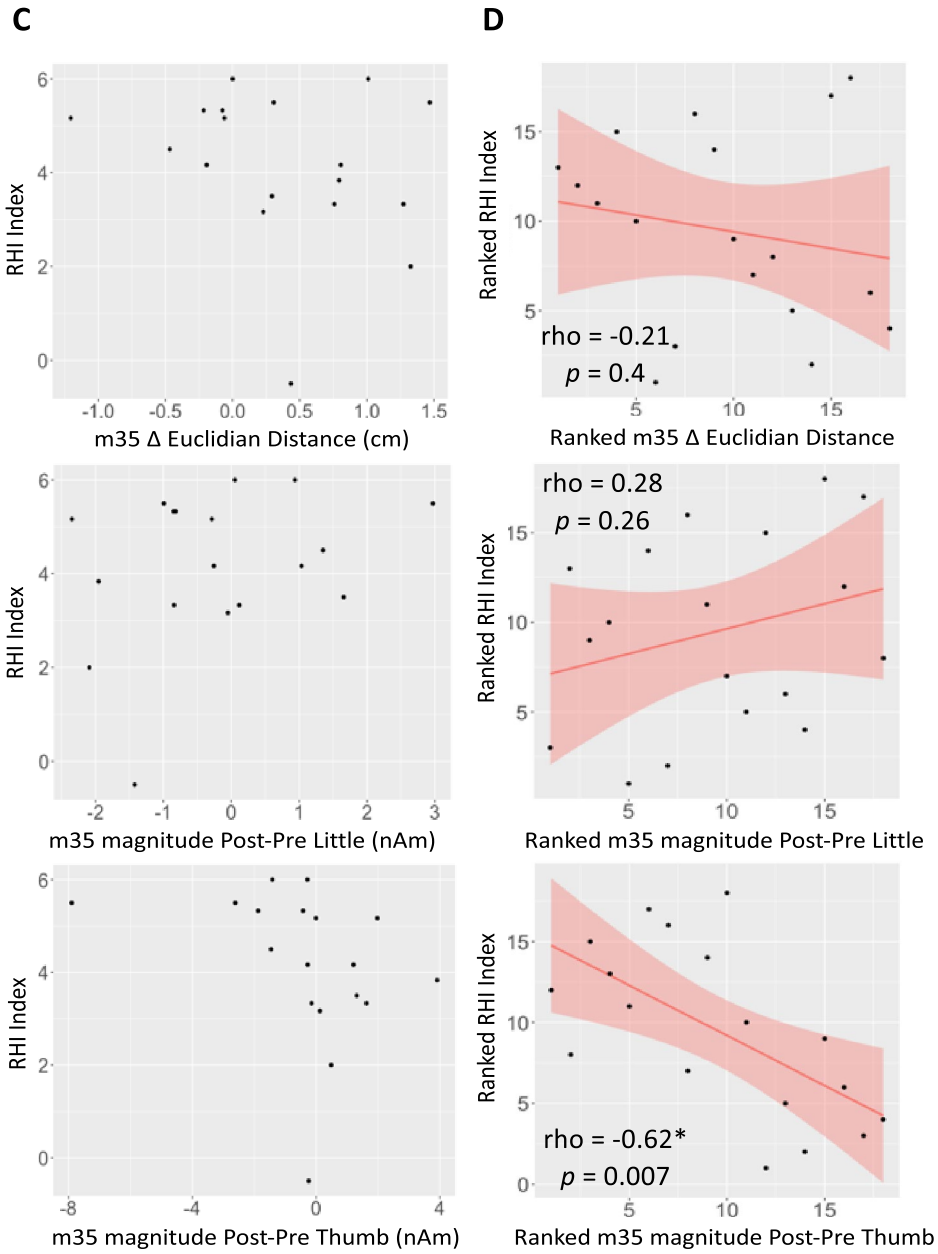

Fig. 6. (continued)

	m20			m35			m45			
	Δ ED	mag. Little	mag. Thumb	Δ ED	mag. Little	mag. Thumb	Δ ED	mag. Little	mag. Thumb	
RHI index	0.49	-0.61	0.01	-0.21	0.28	-0.62	-0.15	0.08	0.02	rho
	0.02	0.008	0.97	0.2	0.26	0.007	0.28	0.77	0.93	p-value

Table 3. Matrix of Spearman's rank correlations, comparing the RHI Index with the Pre-Post change in Euclidian Distance (Δ ED), and the average change in peak magnitude (mag.), as in Fig. 6. Rho indicates the strength of correlation between ranked data, and the *p*-value indicates the significance of the correlation. Cells are colour-coded for strength of values (red for moderate correlation, light yellow for low, the *p*-value cell is yellow for significant correlation).

These shifts are thought to exploit existing peripheral-S1 anatomical connections that remain functionally inactive under usual circumstances[17,66], similar to the early neuroplastic changes that are known to follow amputation[2]. It is unknown whether there are any differences in the underlying mechanisms across m20 and m35 SEF displacements. The source of the m20 in BA3b, the m27 in motor areas (BA4 and BA6), m35 in BA3b and BA1, and m45 in BA1 is in line with known generators of these signals[18,67]. With respect to the current findings that the m35 was localized either to BA3b (Little) or BA1 (Thumb), it is known that for this component, there is higher inter-individual variability and possibly multiple contributing sources[55,56,68], likely reflecting a transition point with respect to inputs to BA3b and BA1. BA1 is known to receive direct thalamocortical inputs as well as inputs from BA3b[69]. Thus, the m35 component likely reflects a transition towards relatively more top-down processing.

The RHI is dependent upon the integration of visual, tactile, and proprioceptive information, which highlights the importance of top-down processes in shaping body ownership and embodiment. The observation that the m35 displacement is posteriorward towards BA1 suggests the importance of visual-tactile integration in the embodiment of the fake hand (i.e.,[23]), which however is not directly related to inter-individual differences in the extent of embodiment. This is a rather intriguing finding, suggesting that this integration is not related to the extent of embodiment, but to some other component of the illusion, for example its initiation or its stability over time.

We did not expect to see shifts or correlations for the very first component (m20), as seen by Rossini and colleagues with decreased use[17]. Our finding that the m20 displacement correlated between-subjects with the extent of embodiment would suggest, beyond the expected effects of top-down integrative processes, that relatively more bottom-up processes related to low-level physical representation are central to embodiment in RHI. Although top-down processes are necessary for the RHI to take hold[24], these results suggest that processes preceding somatosensory integration may have an even more important role. The m20 component in BA3b is thought to reflect cortical relay encoding tactile features limited to individual digits, prior to integration across digits and across sensory modalities (such as with vision).

An alternative explanation is also possible. The changes here were observed after the RHI, i.e., after any plastic changes due to the illusion are likely to have occurred. This leaves the possibility that neuronal correlates of the m20 are indeed influenced by top-down processes due to the RHI. Although these top-down processes are then not active during SEF stimulation, they could have acted in the sense of a "recalibration" as an adaptation of local circuits due to, for example, expectation.

Rubber hand illusion strength is associated with attenuated somatosensory evoked fields

Although we did not observe significant within-subject reduction in SEF magnitude for any of the measured components, we found that the extent of SEF magnitude reduction for individual digits across m20 and m35 components correlated with the RHI index *between-subjects*. Both correlations were in the same direction, demonstrating that subjects who experienced a greater sense of embodiment of the rubber hand had a subsequent greater reduction in SEF magnitude, for the Little at m20 and for the Thumb at m35. We did not expect to find any differences across digits. A possible explanation for this finding comes from a recent study that observed within BA3b of S1 a homogeneous 3D structural architecture between digits 2–5, excluding the thumb[70]. Greater independence of the thumb has also been observed within area 3b of macaque monkeys[71]. It is unlikely that this independence holds for BA1, where integration across fingers is known to occur. Thus, it is possible that our findings of a relationship between embodiment and reduction in magnitude for the Little at the m20 within BA3b reflects this greater predisposition for inter-finger plasticity, excluding the thumb. Meanwhile, since integration is fundamental to BA1, it is unlikely that the thumb retains its independence, and thus thumb-related plastic effects may be more evident here during the m35.

These findings confirm and extend the main findings of previous studies that measured the effect of the RHI on early SEP components and found a reduction in magnitude at similar latencies as the m45 measured in the current study[11], and also when combining earlier latencies that span the 20–25 ms time range[43], thought to originate across BA3b and BA1. Differences between the current results and those of the two aforementioned studies could be due to differences in recording methods, or differences in timing: the aforementioned studies recorded SEPs during the RHI, whereas in the current study the SEFs were recorded before and after the RHI. This is an important distinction, as it is possible that the reduction in SEF magnitude, especially for the m45 component observed by Zeller and colleagues[11], may be a transient effect. Whereas the observations of this study might represent more stable effects of embodiment, lasting beyond the illusion itself.

Possible mechanisms underlying changes to cortical somatosensory finger representation

Given the theory that S1 must be suppressed to prioritize visual information in order for the RHI to occur (e.g.[1]), one might expect the Euclidian distances between digits to contract during the RHI. This is based on findings that somatosensory cortical plasticity related to disuse is typically associated with a contraction of unused digit representations[17,72] and increased use is conversely associated with an expansion of an overused digit's representation[29,73]. However, it is possible that the RHI results in a contraction of somatosensory representation of the stimulated finger only, with a corresponding expansion of the "spared" fingers[74]. This is supported by the findings that for synchronously co-stimulated fingers, their cortical representations contracted, whereas for asynchronously co-stimulated fingers, their cortical representations were centred further apart[75–78], as observed in the current study (thumb and little fingers were asynchronously stimulated). Furthermore, while the RHI increases arousal[59,79], arousal in turn increases cortical inhibition, resulting in less overlap in cortical receptive fields, along with reduced strength of the thalamocortical connection[80]. In this way, a stronger embodiment

during the RHI may be related to a simultaneous increase in Euclidian distance between fingers not involved in the RHI, with a reduction in the strength of thalamocortical input, as observed in this study.

We have considered alternative explanations for the observed correlation between a reduction in SEF magnitude and RHI-Index across subjects. First, instead of a reduction in strength of thalamocortical input, it is possible that this correlation reflects a local and short-term synchronization with respect to input to the cortex related to the rubber hand, resulting in a desynchronization of bottom-up input to the real digits. The synchronization of cortical SEFs could in future be disentangled from total cortical activity with single-trial analysis of these signals. A second possibility is that these changes may be partially driven by top-down influences. For example, activity within the premotor cortex has been linked with the RHI[81], as well as with vicarious somatosensory experience (that is, first-person experience of others' events) following embodiment[82]. Since the premotor cortex has been shown to drive changes in S1 through direct corticocortical connections[83], it is likely that the effects of embodying the rubber hand include bottom-up thalamocortical inputs to S1 as well as top-down inputs from the premotor cortex.

The integration of top-down and bottom-up influences in the RHI has been used to interpret this phenomenon within the framework of a Bayesian causal inference model[84]. During the RHI, the sensory conflict induced by the experimental setup underscores the significance of multisensory integration in body perception. This process is believed to operate on the principle of sensory weighting according to its epistemic value[85]. Multisensory integration can be understood as the resolution of conflicts between sensory inputs, by evaluating the precision of each sensory source. Furthermore, it has been demonstrated that the brain combines different inputs up to a certain degree of incongruence[86], but it stops this integration when the inputs become too uncorrelated[87]. This mechanism is considered to be based on hierarchical computational messaging between lower-level areas, which handle rapidly changing physical aspects of perception and action, and higher-level multisensory areas, which integrate and process more slowly changing, abstract representations of the body and its interaction with the environment[88]. In particular, the posterior parietal cortex, which is known to receive inputs from S1, was involved in the implementation of Bayesian causal inference of body ownership related to the elicitation of the RHI[89]. As far as how our findings contribute to these recent models, we speculate that the displacements we observed in S1 provide may serve as feedforward inputs to the posterior parietal cortex. That is, the modifications to S1 organization that we observed following the RHI may serve as the updated sensory input to update the internal model of the Bayesian causal inference of body ownership, thought to occur within the posterior parietal cortex. Thus, the outcome of the displacements we observed in S1 could be to influence the perceptual decisions and update the body schema within the posterior parietal cortex.

A note on the motor cortex: inversion across the central sulcus

It was not surprising to observe a strong m27 component in precentral motor areas (BA4 and BA6), as this is a known SEF component. However, the discrepancy in source localization results between Little and Thumb responses was not expected. Given the estimated placement of the Little sources on the crown of the precentral gyrus, it is possible that the anatomical layout of the hand representation area results in the Little source being more radially-oriented for this specific component than the Thumb source, and therefore largely insensible by the MEG gradiometers. That said, it is intriguing that the estimated relative layout is in the opposite orientation with respect to the S1 sources. That is, the Little source is estimated to be *more lateral* than the Thumb source in the motor areas, but more medial than the Thumb source in S1. These findings are in line with traditional anatomical layouts of the sensory homunculus, as well as with recent updates to the motor homunculus, including a fMRI study demonstrating concentric medial–lateral representations for the fingers and thumb in the motor cortex, with the Little finger at the centre[64]. Thus, it is not anatomically incorrect for the Thumb source to be medial to the Little source within the motor cortex, as it has representations both medial and lateral to the Little source. With respect to the double representation of the Thumb in the recent motor homunculus, we are intrigued by the current results showing that the medial Thumb representation was stronger than the lateral representation, suggesting a functional difference between these repeated motor cortical Thumb representation areas.

Implications

These findings hold significant practical implications. Specifically, the observed changes in both amplitude and brain localization of the evoked cortical response to somatosensory stimulation could serve as quantitative physiological measurement of limb embodiment. This could be especially useful within the context of treatment or rehabilitation for various neurological and psychiatric conditions characterized by altered body representations, such as stroke with hemiparesis or neglect, eating disorders, body dysmorphic disorder, or prosthetic use. Furthermore, our discoveries could advance the understanding of neurophysiological effects on limb embodiment in these conditions, potentially guiding new therapeutic methodologies. For example, innovative neuromodulation techniques targeting S1 could be explored to enhance prosthetic embodiment, thereby improving motor control and mitigating the altered body image experienced by amputees. This would have the effect of increasing the acceptance and efficacy of prosthetic devices.

Limitations

There are limitations to the current study. We did not measure SEFs immediately before and after RHI control sessions, as the induction of the observed effects to the SEF in the Post condition would invalidate any subsequent SEF procedures, and we did not have the possibility to have subjects return on a different day. This could be the focus of additional studies. As such, our conclusions are strengthened by the correlations between the neuromagnetic data with the RHI index measure. In this way we ensure that our findings are not due to unintended factors such as time, fatigue, or repeated stimulation. Furthermore, since it is known that repeated stimulation

increases the magnitude of SEFs only at long latencies and does not affect the early components analyzed here[90], we do not believe that our results are solely due to repeated paintbrush stimulation during the synchronous RHI, separate from the illusion itself.

Summary and conclusions

The present study demonstrated that the RHI induced changes in the source localization of early SEF components in S1, distinguishing between components and suggested multiple functions of SEF source displacements. The extent of rubber hand embodiment was associated with a between-subject increased distance between Little and Thumb cortical somatosensory representation areas for the m20, and peak magnitude of the m20 and the m35 components for the Little and Thumb, respectively.

These findings contribute to our understanding of the neuroplastic changes underlying successful artificial hand embodiment and provide insights into its potential mechanisms, separate from the neuroplasticity induced by loss of function. Adaptations in S1 accompanying embodiment likely represent different and complex mechanisms compared with use and disuse.

Understanding the neuroplastic changes involved in artificial limb embodiment is crucial for the development of effective strategies to enhance the functionality and acceptance of prosthetic devices, and reduce the occurrence of phantom limb pain. Future research could further investigate the temporal dynamics of somatosensory processing during artificial limb embodiment and explore the relationship between neuroplastic changes and long-term prosthetic use and phantom limb pain, in amputees.

Data availability

All anonymized data will be made available upon reasonable request to GDP (G.DiPino@unicampus.it).

Received: 6 June 2024; Accepted: 6 September 2024
Published online: 27 September 2024

References

1. Castro, F. *et al.* From rubber hands to neuroprosthetics: Neural correlates of embodiment. *Neurosci. Biobehav. Rev.* **153**, 105351 (2023).
2. Di Pino, G., Guglielmelli, E. & Rossini, P. M. Neuroplasticity in amputees: Main implications on bidirectional interfacing of cybernetic hand prostheses. *Prog. Neurobiol.* **88**, 114–126 (2009).
3. Salminger, S. *et al.* Current rates of prosthetic usage in upper-limb amputees-have innovations had an impact on device acceptance?. *Disabil. Rehabil.* **44**, 3708–3713 (2022).
4. Murray, C. D. Embodiment and Prosthetics. In *Psychoprosthetics* (eds Gallagher, P. *et al.*) 119–129 (Springer, 2008).
5. Cuberovic, I., Gill, A., Resnik, L. J., Tyler, D. J. & Graczyk, E. L. Learning of artificial sensation through long-term home use of a sensory-enabled prosthesis. *Front. Neurosci.* https://doi.org/10.3389/fnins.2019.00853 (2019).
6. Di Pino, G. *et al.* Sensory- and action-oriented embodiment of neurally-interfaced robotic hand prostheses. *Front. Neurosci.* https://doi.org/10.3389/fnins.2020.00389 (2020).
7. Fritsch, A., Lenggenhager, B. & Bekrater-Bodmann, R. Prosthesis embodiment and attenuation of prosthetic touch in upper limb amputees–a proof-of-concept study. *Conscious. Cogn.* **88**, 103073 (2021).
8. Pinardi, M. *et al.* Doublecheck: A sensory confirmation is required to own a robotic hand, sending a command to feel in charge of it. *Cogn. Neurosci.* **11**, 216–228 (2020).
9. Isayama, R. *et al.* Rubber hand illusion modulates the influences of somatosensory and parietal inputs to the motor cortex. *J. Neurophysiol.* **121**, 563–573 (2019).
10. Shokur, S. *et al.* Expanding the primate body schema in sensorimotor cortex by virtual touches of an avatar. *Proc. Natl. Acad. Sci.* **110**, 15121–15126 (2013).
11. Zeller, D., Litvak, V., Friston, K. J. & Classen, J. Sensory processing and the rubber hand illusion—an evoked potentials study. *J. Cognit. Neurosci.* **27**, 573–582 (2015).
12. Savolainen, P. *et al.* Facilitation of tactile working memory by top-down suppression from prefrontal to primary somatosensory cortex during sensory interference. *Behav. Brain Res.* **219**, 387–390 (2011).
13. Dykes, R. W. & Metherate, R. Sensory cortical reorganization following peripheral nerve injury. In *Brain injury and recovery: theoretical and controversial issues* (eds Finger, S. *et al.*) 215–234 (Springer, Boston, 1988).
14. Kaas, J. H., Merzenich, M. M. & Killackey, H. P. The reorganization of somatosensory cortex following peripheral nerve damage in adult and developing mammals. *Ann. Rev. Neurosci.* **6**, 325–356 (1983).
15. Makin, T. R., Scholz, J., Henderson Slater, D., Johansen-Berg, H. & Tracey, I. Reassessing cortical reorganization in the primary sensorimotor cortex following arm amputation. *Brain* **138**, 2140–2146 (2015).
16. Pellegrino, G. *et al.* Inter-hemispheric coupling changes associate with motor improvements after robotic stroke rehabilitation. *Restor. Neurol. Neurosci.* **30**, 497–510 (2012).
17. Rossini, P. M. *et al.* Short-term brain 'plasticity'in humans: transient finger representation changes in sensory cortex somatotopy following ischemic anesthesia. *Brain Res.* **642**, 169–177 (1994).
18. Allison, T. *et al.* Human cortical potentials evoked by stimulation of the median nerve. I. Cytoarchitectonic areas generating short-latency activity. *J. Neurophysiol.* **62**, 694–710 (1989).
19. Besle, J., Sánchez-Panchuelo, R.-M., Bowtell, R., Francis, S. & Schluppeck, D. Event-related fMRI at 7T reveals overlapping cortical representations for adjacent fingertips in S1 of individual subjects. *Human Brain Map.* **35**, 2027–2043 (2014).
20. Burton, H. & Fabri, M. Ipsilateral intracortical connections of physiologically defined cutaneous representations in areas 3b and 1 of macaque monkeys: Projections in the vicinity of the central sulcus. *J. Comp. Neurol.* **355**, 508–538 (1995).
21. Macerollo, A., Brown, M. J. N., Kilner, J. M. & Chen, R. Neurophysiological changes measured using somatosensory evoked potentials. *Trends Neurosci.* **41**, 294–310 (2018).
22. Martuzzi, R., van der Zwaag, W., Farthouat, J., Gruetter, R. & Blanke, O. Human finger somatotopy in areas 3b, 1, and 2: A 7T fMRI study using a natural stimulus. *Human Brain Map.* **35**, 213–226 (2014).
23. Rosenthal, I. A. *et al.* S1 represents multisensory contexts and somatotopic locations within and outside the bounds of the cortical homunculus. *Cell Rep.* **42**, 112312 (2023).
24. Tsakiris, M. & Haggard, P. The rubber hand illusion revisited: visuotactile integration and self-attribution. *J. Exp. Psychol. Hum. Percept. Perform.* **31**, 80–91 (2005).

25. Desmedt, J. E., Huy, N. T. & Bourguet, M. The cognitive P40, N60 and P100 components of somatosensory evoked potentials and the earliest electrical signs of sensory processing in man. *Electroencephalogr. Clin. Neurophysiol.* **56**, 272–282 (1983).
26. Hillyard, S. A. & Kutas, M. Electrophysiology of cognitive processing. *Annu. Rev. Psychol.* **34**, 33–61 (1983).
27. Wu, D., Xiong, W., Jia, X., Geocadin, R. G. & Thakor, N. V. Short- and long-latency somatosensory neuronal responses reveal selective brain injury and effect of hypothermia in global hypoxic ischemia. *J. Neurophysiol.* **107**, 1164–1171 (2012).
28. Schaefer, M., Heinze, H.-J. & Rotte, M. My third arm: Shifts in topography of the somatosensory homunculus predict feeling of an artificial supernumerary arm. *Human Brain Map.* **30**, 1413–1420 (2009).
29. Elbert, T., Pantev, C., Wienbruch, C., Rockstroh, B. & Taub, E. Increased cortical representation of the fingers of the left hand in string players. *Science* **270**, 305–307 (1995).
30. Carter, B. G. & Butt, W. Review of the use of somatosensory evoked potentials in the prediction of outcome after severe brain injury. *Crit. Care Med.* **29**, 178–186 (2001).
31. Mauguière, F. Chapter 5 Somatosensory Evoked Responses. In *Handbook of Clinical Neurophysiology* Vol. 1 45–75 (Elsevier, 2003).
32. Mauguière, F., Desmedt, J. E. & Courjon, J. Astereognosis and dissociated loss of frontal or parietal components of somatosensory evoked potentials in hemispheric lesions: Detailed correlations with clinical signs and computerized tomographic scanning. *Brain* **106**, 271–311 (1983).
33. D'Alonzo, M., Clemente, F. & Cipriani, C. Vibrotactile stimulation promotes embodiment of an alien hand in amputees with phantom sensations. *IEEE Trans. Neural Syst. Rehabil. Eng.* **23**, 450–457 (2015).
34. Ehrsson, H. H. *et al.* Upper limb amputees can be induced to experience a rubber hand as their own. *Brain A J. Neurol.* **131**, 3443–3452 (2008).
35. Schmalzl, L., Kalckert, A., Ragnö, C. & Ehrsson, H. H. Neural correlates of the rubber hand illusion in amputees: A report of two cases. *Neurocase* **20**, 407–420 (2014).
36. Ehrsson, H. H., Spence, C. & Passingham, R. E. That's my hand! activity in premotor cortex reflects feeling of ownership of a limb. *Science* **305**, 875–877 (2004).
37. Lloyd, D. M. Spatial limits on referred touch to an alien limb may reflect boundaries of visuo-tactile peripersonal space surrounding the hand. *Brain Cogn.* **64**, 104–109 (2007).
38. Botvinick, M. & Cohen, J. Rubber hands 'feel' touch that eyes see. *Nature* **391**, 756–756 (1998).
39. Armel, K. C. & Ramachandran, V. S. Projecting sensations to external objects: Evidence from skin conductance response. *Proc. R. Soc. Lond. Ser. B Biol. Sci.* **270**, 1499–1506 (2003).
40. Kanayama, N., Sato, A. & Ohira, H. Crossmodal effect with rubber hand illusion and gamma-band activity. *Psychophysiology* **44**, 392–402 (2007).
41. Press, C., Heyes, C., Haggard, P. & Eimer, M. Visuotactile learning and body representation: an ERP study with rubber hands and rubber objects. *J. Cogn. Neurosci.* **20**, 312–323 (2008).
42. Hari, R., Hamalainen, M., Kaukoranta, E., Reinikainen, K. & Teszner, D. Neuromagnetic responses from the second somatosensory cortex in man. *Acta Neurol. Scand.* **68**, 207–212 (1983).
43. Sakamoto, M. & Ifuku, H. Attenuation of sensory processing in the primary somatosensory cortex during rubber hand illusion. *Sci. Rep.* **11**, 7329 (2021).
44. Hämäläinen, M., Hari, R., Ilmoniemi, R. J., Knuutila, J. & Lounasmaa, O. V. Magnetoencephalography—theory, instrumentation, and applications to noninvasive studies of the working human brain. *Rev. Mod. Phys.* **65**, 413–497 (1993).
45. Hedrich, T., Pellegrino, G., Kobayashi, E., Lina, J. M. & Grova, C. Comparison of the spatial resolution of source imaging techniques in high-density EEG and MEG. *NeuroImage* **157**, 531–544 (2017).
46. World Medical Association. World medical association declaration of Helsinki: Ethical principles for medical research involving human subjects. *JAMA* **310**, 2191–2194 (2013).
47. Oldfield, R. C. The assessment and analysis of handedness: The Edinburgh inventory. *Neuropsychologia* **9**, 97–113 (1971).
48. Abdulkarim, Z. & Ehrsson, H. H. No causal link between changes in hand position sense and feeling of limb ownership in the rubber hand illusion. *Attention Percept. Psychophys.* **78**, 707–720 (2016).
49. D'Alonzo, M., Mioli, A., Formica, D., Vollero, L. & Di Pino, G. Different level of virtualization of sight and touch produces the uncanny valley of avatar's hand embodiment. *Sci. Rep.* **9**, 19030 (2019).
50. Tadel, F., Baillet, S., Mosher, J. C., Pantazis, D. & Leahy, R. M. Brainstorm: A user-friendly application for MEG/EEG analysis. *Comput. Intell. Neurosci.* **2011**, 879716 (2011).
51. Lalancette, M., Quraan, M. & Cheyne, D. Evaluation of multiple-sphere head models for MEG source localization. *Phys. Med. Biol.* **56**, 5621–5635 (2011).
52. Jobst, C., Ferrari, P., Isabella, S. & Cheyne, D. BrainWave: A matlab toolbox for beamformer source analysis of MEG data. *Front. Neurosci.* **12**, 587 (2018).
53. Cheyne, D., Bakhtazad, L. & Gaetz, W. Spatiotemporal mapping of cortical activity accompanying voluntary movements using an event-related beamforming approach. *Human Brain Map.* **27**, 213–229 (2006).
54. Cheyne, D., Bostan, A. C., Gaetz, W. & Pang, E. W. Event-related beamforming: a robust method for presurgical functional mapping using MEG. *Clin. Neurophysiol. Off. J. Int. Federation Clin. Neurophysiol.* **118**, 1691–1704 (2007).
55. Kawamura, T. *et al.* Neuromagnetic evidence of pre- and post-central cortical sources of somatosensory evoked responses. *Electroencephalogr. Clin. Neurophysiol. Evoked Potentials Sect.* **100**, 44–50 (1996).
56. Huttunen, J., Komssi, S. & Lauronen, L. Spatial dynamics of population activities at S1 after median and ulnar nerve stimulation revisited: An MEG study. *NeuroImage* **32**, 1024–1031 (2006).
57. Papadelis, C., Eickhoff, S. B., Zilles, K. & Ioannides, A. A. BA3b and BA1 activate in a serial fashion after median nerve stimulation: Direct evidence from combining source analysis of evoked fields and cytoarchitectonic probabilistic maps. *NeuroImage* **54**, 60–73 (2011).
58. Team, R. C. R: A language and environment for statistical com-puting. *R Foundation for Statistical Computing, Vienna, Austria. URL* https://www.R-project.org *(2017).*
59. D'Alonzo, M., Mioli, A., Formica, D. & Di Pino, G. Modulation of body representation impacts on efferent autonomic activity. *J. Cogn. Neurosci.* **32**, 1104–1116 (2020).
60. Buchner, H. *et al.* Somatotopy of human hand somatosensory cortex revealed by dipole source analysis of early somatosensory evoked potentials and 3D-NMR tomography. *Electroencephalogr. Clin. Neurophysiol. Evoked Potentials Sect.* **96**, 121–134 (1995).
61. Wood, C. C. *et al.* Localization of human sensorimotor cortex during surgery by cortical surface recording of somatosensory evoked potentials. *J. Neurosurg.* **68**, 99–111 (1988).
62. Roux, F.-E., Djidjeli, I. & Durand, J.-B. Functional architecture of the somatosensory homunculus detected by electrostimulation. *J. Physiol.* **596**, 941–956 (2018).
63. Hari, R. *et al.* Functional organization of the human first and second somatosensory cortices: A neuromagnetic study. *Eur. J. Neurosci.* **5**, 724–734 (1993).
64. Huber, L. *et al.* Sub-millimeter fMRI reveals multiple topographical digit representations that form action maps in human motor cortex. *Neuroimage* **208**, 116463 (2020).
65. Nakamura, A. *et al.* Somatosensory homunculus as drawn by MEG. *NeuroImage* **7**, 377–386 (1998).
66. Sanes, J. N., Suner, S., Lando, J. F. & Donoghue, J. P. Rapid reorganization of adult rat motor cortex somatic representation patterns after motor nerve injury. *Proc. Natl. Acad. Sci.* **85**, 2003–2007 (1988).

67. Balzamo, E., Marquis, P., Chauvel, P. & Régis, J. Short-latency components of evoked potentials to median nerve stimulation recorded by intracerebral electrodes in the human pre- and postcentral areas. *Clin. Neurophysiol.* **115**, 1616–1623 (2004).
68. Peterson, N. N., Schroeder, C. E. & Arezzo, J. C. Neural generators of early cortical somatosensory evoked potentials in the awake monkey. *Electroencephalogr. Clin. Neurophysiol. Evoked Potentials Sect.* **96**, 248–260 (1995).
69. Jones, E. G., Coulter, J. D. & Hendry, S. H. C. Intracortical connectivity of architectonic fields in the somatic sensory, motor and parietal cortex of monkeys. *J. Comp. Neurol.* **181**, 291–347 (1978).
70. Doehler, J. *et al.* The 3D structural architecture of the human hand area is nontopographic. *J. Neurosci.* **43**, 3456–3476 (2023).
71. Lazar, L., Chand, P., Rajan, R., Mohammed, H. & Jain, N. Somatosensory cortex of macaque monkeys is designed for opposable thumb. *Cereb. Cortex* **33**, 195–206 (2023).
72. Elbert, T. *et al.* Alteration of digital representations in somatosensory cortex in focal hand dystonia. *NeuroReport* **9**, 3571–3575 (1998).
73. Godde, B., Ehrhardt, J. & Braun, C. Behavioral significance of input-dependent plasticity of human somatosensory cortex. *NeuroReport* **14**, 543–546 (2003).
74. Feldman, D. E. & Brecht, M. Map plasticity in somatosensory cortex. *Science* **310**, 810–815 (2005).
75. Braun, C. *et al.* Activity patterns of human somatosensory cortex adapt dynamically to stimulus properties. *NeuroReport* **11**, 2977 (2000).
76. Pilz, K., Veit, R., Braun, C. & Godde, B. Effects of co-activation on cortical organization and discrimination performance. *NeuroReport* **15**, 2669 (2004).
77. Vidyasagar, R., Folger, S. E. & Parkes, L. M. Re-wiring the brain: Increased functional connectivity within primary somatosensory cortex following synchronous co-activation. *NeuroImage* **92**, 19–26 (2014).
78. Ziemus, B. *et al.* Effects of passive tactile co-activation on median ulnar nerve representation in human S1. *NeuroReport* **11**, 1285 (2000).
79. Di Pino, G., Mioli, A., Altamura, C. & D'Alonzo, M. Embodying an artificial hand increases blood flow to the investigated limb. *Open Res. Eur.* **1**, 55 (2022).
80. Castro-Alamancos, M. A. Dynamics of sensory thalamocortical synaptic networks during information processing states. *Prog. Neurobiol.* **74**, 213–247 (2004).
81. Chancel, M., Iriye, H. & Ehrsson, H. H. Causal inference of body ownership in the posterior parietal cortex. *J. Neurosci.* **42**, 7131–7143 (2022).
82. Pamplona, G. S. P. *et al.* Illusory body ownership affects the cortical response to vicarious somatosensation. *Cereb. Cortex* **32**, 312–328 (2021).
83. Zagha, E., Casale, A. E., Sachdev, R. N. S., McGinley, M. J. & McCormick, D. A. Motor cortex feedback influences sensory processing by modulating network state. *Neuron* **79**, 567–578 (2013).
84. Samad, M., Chung, A. J. & Shams, L. Perception of body ownership is driven by bayesian sensory inference. *PLOS ONE* **10**, e0117178 (2015).
85. Parr, T. & Friston, K. J. Uncertainty, epistemics and active inference. *J. R. Soc. Interface* **14**, 20170376 (2017).
86. Blanke, O., Slater, M. & Serino, A. Behavioral, neural, and computational principles of bodily self-consciousness. *Neuron* **88**, 145–166 (2015).
87. Rohe, T. & Noppeney, U. Cortical hierarchies perform bayesian causal inference in multisensory perception. *PLoS Biol* **13**, e1002073 (2015).
88. Limanowski, J. What can body ownership illusions tell us about minimal phenomenal selfhood?. *Front. Hum. Neurosci.* **8**, 946 (2014).
89. Chancel, M., Ehrsson, H. H. & Ma, W. J. Uncertainty-based inference of a common cause for body ownership. *eLife* **11**, e77221 (2022).
90. Dowman, R. & Rosenfeld, J. P. Effects of naloxone and repeated stimulus presentation on cortical somatosensory evoked potential (SEP) amplitude in the rat. *Exp. Neurol.* **89**, 9–23 (1985).

Author contributions

SLI: Formal analysis, Visualization, Writing—Original Draft; MDA: Conceptualization, Resources, Writing—Review & Editing; AM: Conceptualization, Data Acquisition, Writing—Review & Editing; GA: Data Acquisition, Resources, Writing—Review & Editing; GP: Data Acquisition, Writing—Review & Editing, Supervision, Funding Acquisition; GDP: Conceptualization, Resources, Writing—Review & Editing, Supervision, Funding Acquisition.

Funding

This study was made possible by support from an Italian Ministry of Health Operating Grant to San Camillo Hospital IRCCS Venice (GR-2019-12368960) to GP, as well as from the European Research Council (RESHAPE ERC-2015-STG) to GDP, from the Italian Ministry of University and Research (Enable R16ZBLF9E3, Propriouss 2022jj8zee) to GDP, from the Italian Worker's Compensation Authority (INAIL: Spine 4.0 c85f21001020001, WiFiMyoHand PEN0138, NoProblem) to GDP.

Competing interests

The authors declare no competing interests.

Additional information

Supplementary Information The online version contains supplementary material available at https://doi.org/10.1038/s41598-024-72460-6.

Correspondence and requests for materials should be addressed to S.L.I.